

**FINAL REPORT
NATURAL BRIDGE INVESTIGATION**

**Chester F. Watts, PhD, CPG
Director, Radford University Geohazards Research Center**

**George C. Stephenson, MS, CPG
FAA Certified Remote Pilot in Command
Radford University Geohazards Research Center**



*Frontispiece/*Figure 1: False-color point-cloud image of Natural Bridge,
Rockbridge County, Virginia.

Geohazards and Unmanned Systems Research Center
Department of Geology, Radford University

Radford, Virginia 24142

April 2018
(VTRC 99584)

DISCLAIMER

The contents of this report reflect the views of the author(s), who are responsible for the facts and the accuracy of the data presented herein. The contents do not necessarily reflect the official views or policies of the Virginia Department of Transportation, the Commonwealth Transportation Board, or the Federal Highway Administration. This report does not constitute a standard, specification, or regulation. Any inclusion of manufacturer names, trade names, or trademarks is for identification purposes only and is not to be considered an endorsement.

Due to the complexity of this study and the great volumes of data that were collected and analyzed over a period of just six months, using twelve different methodologies, this report is intended to provide only an overview of the methods and analytical techniques applied to this investigation, along with a summary of results and conclusions. Anyone wanting access to more extensive data and results, please contact the authors for Internet access to the various project folders.

EXECUTIVE SUMMARY

The Virginia Department of Transportation, in cooperation with the Department of Conservation and Recreation, contracted with the engineering geology group at Radford University to complete a geological and geotechnical investigation of the unique feature known as Natural Bridge. This 90-foot long bedrock formation crosses Cedar Creek Gorge with a base approximately 190 feet above the creek bed and carries U.S. Route 11; Cedar Creek flows beneath and through the part of the formation that carries the highway. It is the only known highway alignment resting on an in-situ, naturally-occurring bedrock formation of this nature. Analyses of the data suggest that the rock formation continues to be safe for vehicular travel. However, the investigation has revealed geological structures, typical of this geological terrane, within the rock mass including: unfavorable joint sets; through-cutting fracture planes; internal voids; water seepage; and sensitive rock slabs and masses, which are susceptible to falling to the trail below. Vibrations from traffic, along with other human influences, such as stormwater concentration, will continue to aggravate the ever-present processes of erosion, weathering, and gravity. While the formation is safe for vehicular traffic in its current configuration, the Virginia Department of Transportation and the Department of Conservation and Recreation plan to ensure that this unique natural resource is protected to the greatest extent possible for the enjoyment of future generations. Due to the engineering geological condition of the rock formation, altering existing stress fields and load conditions by building a manmade bridge over Natural Bridge is not recommended. It is however recommended that vehicular traffic be eventually removed from Natural Bridge, and the two Departments have begun the planning process to study alternative alignments for U.S. Route 11 while maintaining the functionality of the transportation corridor.

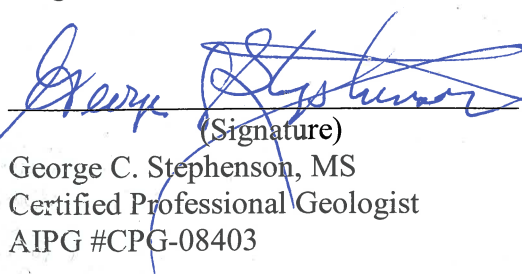


(Signature)

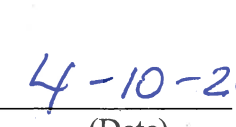
Chester F. Watts, PhD, M.ASCE
Certified Professional Geologist
Virginia #2801000408



(Date)



George C. Stephenson, MS
Certified Professional Geologist
AIPG #CPG-08403



4-10-2018

(Date)

ABSTRACT

Natural Bridge, located in Rockbridge County, Virginia, is a natural limestone rock structure spanning Cedar Creek Gorge. US Route 11, a primary road, crosses Cedar Creek approximately 215 feet above the creek bed via this rock formation. The Virginia Department of Transportation requested an investigation of the geological and geotechnical condition of the rock formation to facilitate decisions regarding safety for the traveling public, aesthetics, and to aid in preserving the natural resource. The investigation was performed by Radford University as contracted by the Virginia Department of Transportation in cooperation with the Department of Conservation and Recreation.

Three aspects of the rock formation related to stability and safety were investigated: (1) internal composition; (2) external shape and features controlled by geological structure; and, (3) vibrations affecting sensitive areas. A variety of geophysical and remote sensing tools and techniques were employed for each aspect. Internal imagery reveals that the natural rock formation contains voids of no great concern to global stability; these are common to bedrock in karst terrane such as this. External imagery reveals that the sides and underside of the formation and gorge include rock slabs that pose localized rock fall hazards to park visitors beneath the formation, and through-cutting rock fractures likely to impact long-term global stability. Analyses of seismometer (vibration sensor) data reveal that vibrations from human sources, including highway traffic, cause portions of the natural rock formation to vibrate and resonate in measurable amounts.

Preliminary analyses suggest that the rock formation itself is safe from global collapse and that there is no danger to the public driving on U.S. Route 11. Safety factor calculations for sensitive rock blocks and rock masses on the sides and underside of the formation and adjacent gorge indicate that rocks of various sizes will continue to fall to the trail from time-to-time, representing potential hazards to park visitors below. Vibrations from both traffic and the sound-and-light show have been modeled mathematically showing that those vibrations can aggravate the natural loss of strength to sensitive areas on the formation and within the gorge.

CONTENTS

EXECUTIVE SUMMARY

ABSTRACT

INTRODUCTION

PURPOSE AND SCOPE

DESCRIPTION OF METHODOLOGIES AND TIMING

1. Electrical Resistivity Imaging
2. Seismic Refraction
3. Multichannel Analysis of Surface Waves (MASW)
4. Ground Penetrating Radar
5. Unmanned Aerial Systems (UAS) Photography and Videography
6. Unmanned Aerial Systems Remote Discontinuity Mapping
7. GigaPan Imaging
8. RU Terrestrial Light Detection and Ranging (LiDAR) for 3D Mapping
9. Manual Discontinuity Mapping
10. Vibration Monitoring
11. Safety Factor Calculations

RESULTS AND DISCUSSION

1. Electrical Resistivity Imaging
2. Seismic Refraction
3. Multichannel Analysis of Surface Waves (MASW)
4. Ground Penetrating Radar
5. Unmanned Aerial Systems (UAS) Photography and Videography
6. Unmanned Aerial Systems Remote Discontinuity Mapping
7. GigaPan Imaging
8. RU Terrestrial Light Detection and Ranging (LiDAR) for 3D Mapping
9. Manual Discontinuity Mapping
10. Vibration Monitoring
11. Local Safety Factor Calculations
12. Global Safety Factor Calculations

SUMMARY OF RESULTS

CONCLUSIONS AND RECOMMENDATIONS

ACKNOWLEDGEMENTS

REFERENCES

APPENDIX – Geophysical Study for Natural Bridge, Rockbridge County, Virginia

BLANK PAGE

**FINAL REPORT
NATURAL BRIDGE INVESTIGATION**

**Chester F. Watts, PhD, PG
Director, Radford University Geohazards Research Center**

**George C. Stephenson, MS, CPG
FAA Certified Remote Pilot in Command
Radford University Geohazards Research Center**

INTRODUCTION

Radford University (RU) is pleased to submit this report on the investigation of Natural Bridge with regard to local and global stability of the Natural Bridge formation in Rockingham County, Virginia.

Geology of Natural Bridge

Natural Bridge is located within the Valley and Ridge physiographic province, close to the boundary between the Blue Ridge and Valley and Ridge physiographic provinces. The region is typified by a dendritic drainage pattern in the Blue Ridge province rocks (the Precambrian Virginia Blue Ridge Complex), changing at the boundary to a trellis pattern controlled by linear ridges, in which Lower Ordovician rock units are exposed (Spencer, 1968). These rocks are nearly horizontal as the result of being part of an open, expansive syncline (Spencer, 1968). The formation itself is believed to be the remnant of a natural tunnel formed along a fracture when the upper portion of Poague Run was captured by Cascade Creek, forming Cedar Creek. This natural tunnel followed the southeasterly regional dip of the strata. As erosion continued, the roof of the passage collapsed, leaving only the rock formation now known as Natural Bridge (Frontispiece/Figure 1 and Figure 2) in a section that was thicker and more resistant to erosion (Spencer, 1968).

The rock formation and valley walls are composed primarily of rock belonging to the lower Ordovician Beekmantown Formation, described as a light gray-colored massive-bedded arenaceous dolomite, which exhibits a strong crosshatch “butcherblock” pattern (Spencer, 1968), commonly seen on weathered surfaces. The dolomite also contains some floating sand grains, cherts, and well-rounded sand grains. The Beekmantown Formation overlies the Chepultepec Formation, the contact being found at the very base of the formation, and visible at the intersection of U.S. 11 and Virginia Route 130, just northeast of the formation. The Chepultepec is described as fine-to-medium grained limestone, which is a bluish gray in color, and contains flat-pebble conglomerates, as well as minor amounts of dolomite and thin-bedded silt (Spencer, 1968).

The rock formation itself is approximately 90 feet long and rises roughly 190 feet above Cedar Creek. The thickness of the formation varies from about 45 to 150 feet, with 50 feet being a common thickness (Spencer, 1968). The formation is shaped by widely spaced joints, which are locally visible. Northeasterly-trending joints form the sides of the formation, whereas the sides of the gorge are formed by north-northwesterly-trending joint sets that intersect additional joint sets trending to the east-southeast. Additional details may be found below.

A serious rock fall event occurred from the underside of the formation of Natural Bridge, Virginia on Saturday, October 23, 1999 resulting in one fatality. A multidisciplinary advisory team, assembled on behalf of the owner of Natural Bridge by Dr. Gary Rogers, examined the formation way as well as approach areas to the underside of the formation that are accessible to the public during operating hours. A report, dated January 20, 2000, written by this author, detailed the resulting investigation of the incident and geological conditions. That report was commissioned by the then-owners of Natural Bridge and is therefore not appended here; however, copies of that report may be made available upon request to this author.

As of the date of this report, the ownership of Natural Bridge is transitioning from private ownership to public ownership. Upon satisfaction of financial considerations, the formation and surrounding areas will be owned and operated as a State Park by the Virginia Department of Conservation and Recreation, with the Commonwealth of Virginia assuming liability and responsibility for this unique geological feature. The Virginia Department of Transportation and the Department of Conservation and Recreation plan to ensure that this resource is protected to the greatest extent possible for the enjoyment of future generations. This is in accordance with the Virginia Department of Transportation's mission, which is to plan, deliver, operate and maintain a transportation system that is safe, enables easy movement of people and goods, enhances the economy and improves our quality of life.

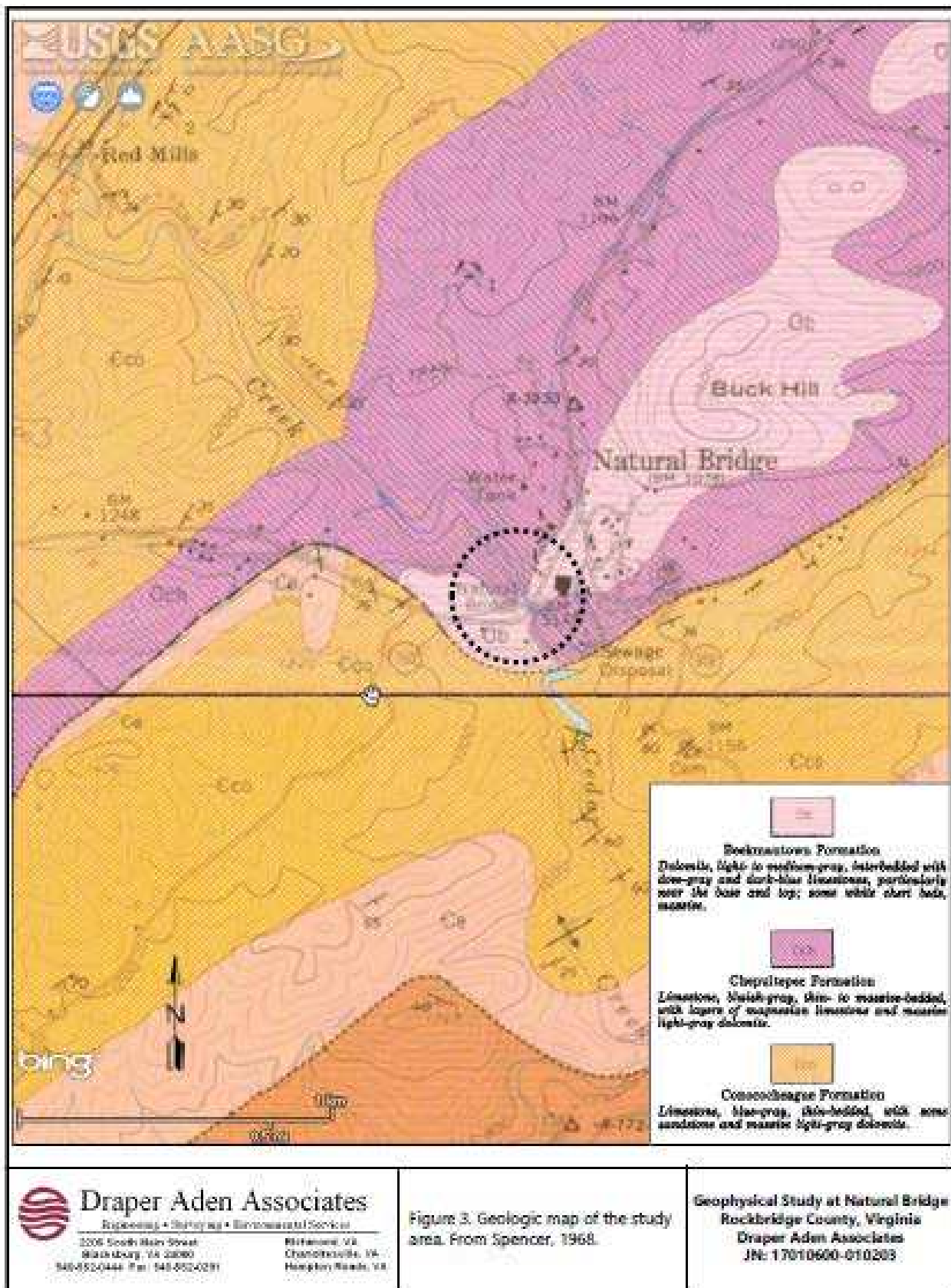


Figure 2: Geological map of Natural Bridge and vicinity. From Draper Aden, 2017; Spencer, 1968

PURPOSE AND SCOPE

The purpose of the study is to examine the geological conditions and structure influencing the stability of the natural rock formation that carries U.S. Route 11 at Natural Bridge, Virginia, and to determine whether or not Route 11, the traffic which travels on Route 11, and vibrations associated with traffic, or from any other sources, have any detrimental impacts on the condition and safety of the natural rock formation.

Due to the poorly-understood geological conditions prior to the date of this report, drilling, invasive investigations, or other potentially damaging methods were specifically not considered; only non-invasive and non-destructive methods were allowed. The scope included the application of a variety of technologies to examine both the internal and external structure of the natural rock formation and to monitor vibrations of the formation and associated sensitive areas caused by traffic and/or other sources, so that the influence of those vibrations on safety and stability could be evaluated by computer modeling. Technologies included electrical resistivity imaging, seismic refraction, multichannel analysis of surface waves, ground penetrating radar, unmanned aerial systems surveys, GigaPan imaging, LiDAR imaging, manual discontinuity mapping, and vibration monitoring using three different types of seismometers (vibration sensors.)

Discontinuities are breaks in the continuity of a rock mass, such as bedding planes, faults, joint sets, and fractures. They provide weak surfaces along which separation, sliding, and falling might generate. They also provide conduits for water flow in ways that can destabilize rock slabs and blocks. Results from this detailed testing provide insight into the stability of the natural rock formation and allow for safety factors to be calculated for sensitive parts of the formation and the surrounding rock gorge.

DESCRIPTION OF METHODOLOGIES AND TIMING

For what is perhaps the most comprehensive evaluation of any natural rock feature in Virginia, eleven or more different technologies were employed to accomplish VDOT's objectives. A list of the most significant methods is provided below, along with their approximate dates of implementation, and brief descriptions of the method type and purpose. All of the methods resulted in mutually consistent interpretations, with no anomalous or conflicting data. All data will be made available online subsequent to the date of this report.

1. Electrical Resistivity Imaging

When: October 3 through 5, 2017

Method Description: Electrical currents are passed between electrodes spread across the ground surface. Resistivity is measured at key locations and computed for various depths, providing a 2D image of subsurface geology and structure.

Method Purpose: Changes in resistivity at various depths provide an indication of the material type (rock, soil, air) and water content. These data allow geological cross-sections and profiles of geological features to be constructed for use in later analyses.

2. Seismic Refraction

When: October 3 through 5, 2017

Method Description: Compressive-type seismic shock waves are introduced into the ground using a hammer device. The waves are refracted while traveling through the geological feature and are recorded by geophones spread across the ground surface. Travel times are recorded at key locations and allow 2D images of subsurface geology and structure to be constructed.

Method Purpose: These tests measure the densities of subsurface material (rock, soil, air) and allow geological cross-sections and profiles of geological features to be constructed for use in later analyses.

3. Multichannel Analysis of Surface Waves (MASW)

When: October 3 through 5, 2017

Method Description: Seismic survey method used to evaluate the elastic stiffness of the ground for geotechnical engineering evaluations. MASW measures seismic surface waves generated using a hammer device and determines subsurface shear-wave velocity variations to complement 2D images generated by seismic refraction methods.

Method Purpose: Shear-wave velocity relates directly to Young's modulus of elasticity. It is often considered to be a direct indicator of ground strength. With computer processing, final MASW information can be provided in 2D and 3D formats.

4. Ground Penetrating Radar (GPR)

When: October 3 through 5, 2017

Method Description: A geophysical method that uses radar signals to create subsurface images. This nondestructive technique sends electromagnetic radiation of the microwave band into the ground and records signals reflected by subsurface structures.

Method Purpose: GPR is capable of detecting rock, soil, ice, fresh water, pavements and structures. It can be used to identify changes in material properties, voids, and cracks.

5. Unmanned Aerial Systems (UAS) Photography and Videography

When: October, 2017 through March, 2018

Method Description: Digital Photogrammetry. High resolution photographs and videos collected using unmanned aerial vehicles (UAVs).

Method Purpose: Provides visual imagery of topographic and structural surface features. Sensors may work in visible, thermal, and infrared ranges. Provides perspectives, not normally visible, that are often enlightening and dramatic.

6. Unmanned Aerial Systems (UAS) Remote Discontinuity Mapping

When: October, 2017 through March, 2018

Method Description: Digital Photogrammetry. High resolution stereoscopic imagery collected using unmanned aerial vehicles (UAVs). Imagery is to be used specifically for generating digital 3D computer models and orthophotomosaics. UAV missions may be manually controlled or pre-programmed remotely.

Method Purpose: 3D computer models may be used to extract geological structure information, including discontinuity orientation data and dimensions used for rock slope

stability analysis. This 3D photogrammetry complements LiDAR mapping and manual discontinuity mapping (see methods #8 and #9 below).

7. GigaPan Imaging

When: December 2, 2017

Method Description: GigaPan uses a tripod-mounted robotic system to control a high resolution camera as it takes overlapping digital images of a subject of interest. Those images are then stitched together to build an interactive detailed representation of the subject. The user can pan left-right and up-down and well as zoom in and out of the finished image.

Method Purpose: GigaPan imagery provides extremely detailed views of rock formations that will reveal underlying geological structure and features that are not immediately visible to the unaided human eye. It can help identify and locate rock discontinuities but does not allow for orientation measurements.

8. Terrestrial Light Detection and Ranging (LiDAR) for 3D Mapping

When: September 2017 (VDOT) and December 2, 2017 (RU)

Method Description: Robotic laser surveying technique providing high resolution 3D digital surface models of manmade structures, terrain, and rock mass features.

Method Purpose: Terrestrial LiDAR surveys provide a three dimensional representation of the geological formation's surface features. This complements the 3D digital surface models from stereo imagery collected using UAS.

9. Manual Discontinuity Mapping

When: October, 2017 through March, 2018

Method Description: Discontinuities are weaknesses, or breaks in the continuity of a rock mass, along which rock slabs or blocks might separate, leading to rock slides or falls. They can also serve as conduits for water flow, leading to potentially detrimental water pressure. Manual discontinuity mapping involves the use of geological pocket transits or smartphone apps to physically measure the orientations of these structural features directly on rock outcrops.

Method Purpose: Orientation data are plotted on stereonets providing kinematic representations of structural weaknesses used to predict potential rock failures. Manual discontinuity mapping is limited to locations physically accessible. Data from manual discontinuity mapping complements data obtained from LiDAR and UAS mapping, which are not limited to locations physically accessible.

10. Vibration Monitoring

When: October, 2017 through March, 2018

Method Description: Vibration sensors are small seismometers (vibration sensors) placed at key locations on the natural rock formation, or the walls of the adjacent gorge, in order to quantify ground vibrations from traffic and other sources. The sensors convert ground motions into electrical signals displayed as seismic waves having measurable amplitudes and frequencies. This study employed three types of sensors: Infilttec QM-4.5V-20HZ vertical seismometers; Radford University Model 03 triaxial seismometers; and VibSensor triaxial seismometer application version 2.0.0 on three iOS smart phones.

Method Purpose: The sensors measure ground vibrations from all sources. This includes

traffic, loudspeakers used for the sound-and-light show, and ambient noise from nearby machinery. Vibration monitoring can indicate whether or not different parts of the rock formation are receiving more vibration than other parts. Importantly, peak accelerations can be determined from the vibration seismograms and used for modeling slope stability safety factors of the formation at sensitive locations.

11. Safety Factor Calculations

When: January through March, 2018

Method Description: Factor of Safety (FS) analysis is an approach to stability evaluation based on determining the ratio of available strength to driving forces or stresses. It is similar to stability evaluation based on shear strength reduction analyses (SSR). In both cases, resisting strengths are compared to driving influences. For example, natural weathering within rock mass discontinuities reduces strength. The pull of gravity, the push of water pressure, and measurable vibrations, serve as examples of driving forces.

Method Purpose: As strength is lost, and/or driving forces are somehow increased over time, rock slopes become less and less stable until failure eventually occurs. Computer software such as RocScience's *Slide* or RockWare's *RockPack III*, can be used to evaluate Factors of Safety. In this study, safety factors are being evaluated taking into account rock formation geometries, geological structure including discontinuity orientations, possible water pressures, strength reduction over time, and the influence of vibrations from traffic and other sources. It should be noted that factor of safety are the results of a mathematical model whose algorithm necessarily includes a range of values due to natural geological variability and variations in observations and measurements; we are confident that the factors of safety noted in this report are based on reliable and repeatable observations and measurement, and reasonable ranges of geological variability.

RESULTS AND DISCUSSION

1. Electrical Resistivity Imaging

Introduction

Electrical resistivity imaging uses an electric current passing through the ground between manually inserted electrodes to create cross-sectional images of the resistance to electric current of subsurface materials. Geological conditions can be inferred from the cross-sections. Values of high resistivity reveal that material is very resistant to the flow of electricity; low values reveal that material transmits electrical current very easily.

This method is very good at identifying underground voids filled with air, as they will have notably high resistivities, as well as underground voids filled with silt and clay, as they will have notably low resistivities. This method is also good for identifying zones of water, and fractures that serve as conduits for water, as those will have notably low values for resistivity. Resistivity imaging also provides estimates of the depth to bedrock beneath soil deposits and artificially placed fill and pavement.

Resistivity imaging was performed in this study to evaluate whether or not there are voids within the natural rock formation, and if so, their approximate locations and relative sizes. A secondary purpose was to provide information regarding variations in the thicknesses of natural soil and artificial fill beneath the pavement crossing the formation. This is useful for evaluating the depth to bedrock and the true thicknesses of the natural rock formation.

Application of the Method

Draper Aden Associates (DAA) of Blacksburg, Virginia performed the resistivity surveys under RU supervision. DAA reports that field data were collected using a SuperSting R8 IP® multi-electrode resistivity system manufactured by Advanced Geosciences Inc. A dipole-dipole array was employed with a current of up to 2000 milliamps. For each electrode configuration in the array, measurements were repeated a minimum of two times, and percent error between the repeated measurements were stored for subsequent evaluation of data quality.

Results of Electrical Resistivity Imaging

The results of the surveys are summarized below and described in detail in the appendix, *Geophysical Study at Natural Bridge*, pages 4 to 9; and, in the accompanying figures shown on pages 37 to 41 in the appendix.

Three resistivity survey lines were established on the pavement of Natural Bridge parallel to the center line. Figure 3 shows the location of the survey lines (top left); the pinnacled appearance of the bedrock outcrops near the south end of the formation (top

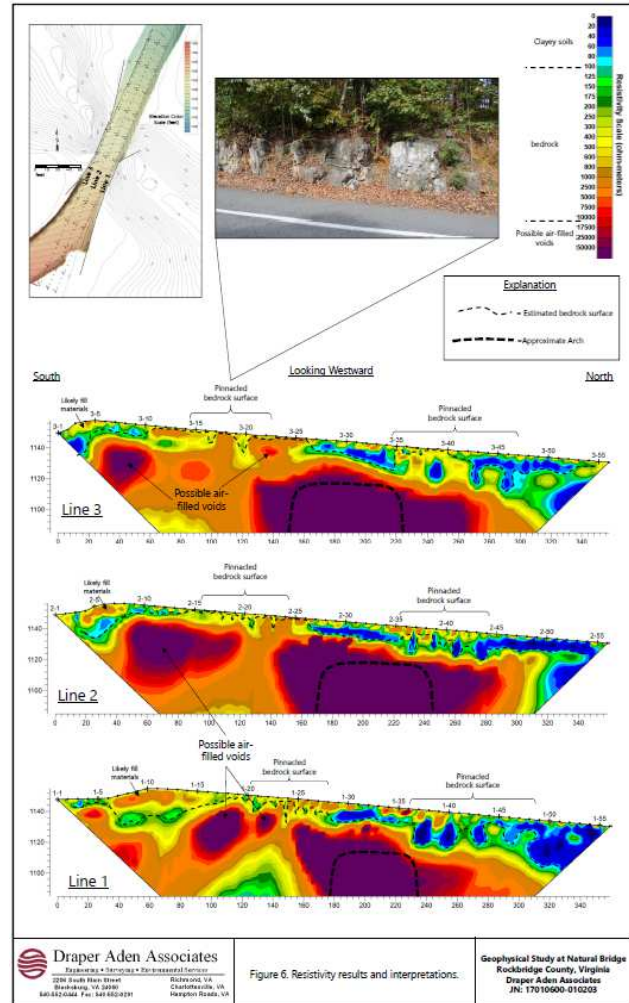
center); and, cross-sectional images of the resistivity data. The following can be deduced from geological interpretations of the resistivity images:

- a. The limestone rock formation itself contains solution cavities, as do the bedrock approaches on either side of the formation. Solution features of varying sizes are common in areas of limestone and are to be expected in this area.
- b. Some of the solution cavities to the south of the formation appear to be air-filled, while others to the north of the formation appear to be sediment-filled. The sedimentary infilling materials are most likely clay-rich, based on the nature of the limestone parent material and on the low resistivity values detected within the voids.
- c. The bedrock surface beneath the pavement appears to have a cutter-and-pinnacle profile, also common in areas of limestone. Cutters are depressions eroded into the bedrock that typically contain infillings of sediment. Pinnacles are erosional bedrock remnants that poke up between cutters.
- d. The presence of the large, probably air-filled, natural void beneath the surface at the south end of the formation, while not affecting the global stability of the formation, will create engineering challenges for the design of a bridge abutment foundation in that vicinity, should a manmade bridge over the rock formation be considered as an alternative.
- e. Analyses of these data indicate that the formation remains safe for the travelling public.

2. Seismic Refraction Imaging

Introduction

Seismic refraction imaging is based on the different velocities with which seismic waves travel through different materials regardless of the seismic source. In this case, a



shock wave is introduced into the ground by striking a metal plate, resting on the surface, with a large hammer. The fastest traveling seismic signals, known as p-waves, consist of a compressional stress that passes through the subsurface material, similar to a sound wave passing through air. It will travel rapidly through hard dense bedrock and slow as it passes through softer soil and fill material.

Geological conditions can be inferred from the cross-sections showing materials of different p-wave velocities. This method is very good at distinguishing between natural soil along with artificial fill and hard bedrock, because of the notably different p-wave velocities. A limitation of seismic refraction is that it works best when materials become denser with depth, hence p-wave velocities increase with depth. Pockets of low velocity will be obscured or invisible in the seismic profiles.

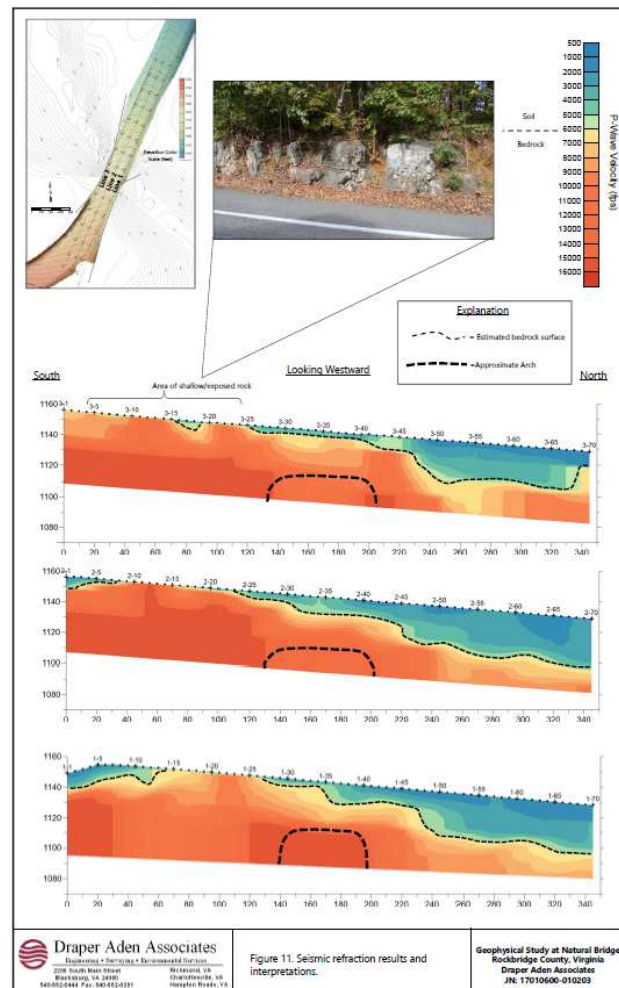
Seismic refraction imaging was performed in this study primarily to evaluate the depth to bedrock beneath the pavement without the need for drilling. A secondary purpose was to provide information regarding the actual bedrock thickness of the rock formation, ignoring the added thickness of natural soil and artificial fill.

Application of the Method

Draper Aden Associates (DAA) of Blacksburg, Virginia performed the seismic refraction surveys. DAA reports that field data were collected using a series of twenty-four 4.5-Hz geophones, spaced 5 feet apart for a total seismic line spread of 115 feet per data set. The geophones were connected via a seismic cable to a Geometrics Geode seismograph. Refraction data were collected from five shot point (energy source) locations located along each spread. The shot point locations were distributed within and beyond the extents of the geophone spread, with a central shot point in the middle of the spread.

Results of Seismic Refraction Imaging

The results of the surveys are summarized below and described in detail in the appendix, *Geophysical Study at Natural Bridge*, pages 10 to



Draper Aden Associates

Engineering • Geoscience • Environmental Services

2028 South Main Street

Blacksburg, VA 24060

540.234.2222 | 800.332.2222

Figure 11. Seismic refraction results and interpretations.

Geophysical Study at Natural Bridge
Rockbridge County, Virginia
Draper Aden Associates
JN 17016060-010203

Figure 4. Location of seismic refraction lines and examples of seismic profiles across Natural Bridge. [From Draper Aden Associates, 2017, Fig. 11.]

13; and, in the accompanying figures shown on pages 42 and 43 in the appendix.

Three seismic refraction lines were established on the pavement of Natural Bridge parallel to the center line as shown in Figure 4. Figure 4 shows the location of the survey lines (top left); the pinnacled appearance of the bedrock outcrops near the south end of the formation (top center); and, cross-sectional images of the seismic data. The following can be deduced from geological interpretations of the seismic refraction images:

- a. The seismic refraction cross-sections reveal pockets of low velocity material (soils and fill) extending downward into bands of high velocity material (bedrock).
- b. These profiles are consistent with those from electrical resistivity imaging, but as expected, voids filled with low velocity material will be obscured by the overlying higher velocity material.
- c. These profiles also indicate the presence of cutter-and-pinnacle karst, consistent with the profiles from electrical resistivity imaging.
- d. Lastly, these profiles show that bedrock rises all the way to the surface on the south side of the formation, which is consistent with observations on-site, where outcrops of limestone appear at the surface.
- e. Analyses of these data indicate that the formation remains safe for the travelling public.

3. Multichannel Analysis of Surface Waves (MASW)

Discussion and Results

The MASW method measures the shear wave (s) velocity of materials, rather than compressional wave (p) velocities, as in the seismic refraction method. Under normal circumstances, MASW can provide a profile of velocity versus depth. Vertical changes in shear wave velocity may be used to evaluate the vertical heterogeneity of subsurface materials. MASW uses the propagation of an elastic wave through the ground, usually induced by a blow from a hammer or drop-weight as with seismic refraction.

Widespread use of MASW began in the early 2000's, primarily as a way to evaluate the likely behavior of manmade structures subject to earthquake vibrations. Radford University requested that Draper Aden Associates employ MASW at Natural Bridge as a test of its effectiveness related to vibration behavior of rock structures over subsurface voids. To our knowledge, this is the first time MASW was applied to a narrow rock formation spanning a gorge.

Draper Aden Associates stated in personal communication that MASW provided reasonable results over the bedrock approach to the rock formation. However, they also report that the data sets and results became severely degraded as the center point of each spread approached the formation. This can be attributed to the large difference in shear wave velocity between the rock of the formation and the air beneath the formation, with a velocity of essentially zero. In light of the above, MASW provides little information of

help in regard to specifically evaluating short-term or long-term stability of Natural Bridge; it did, however, complement and agree with the results of the resistivity survey described above, particularly at the areas away from the air-filled void beneath U.S. Route 11.

4. Ground Penetrating Radar (GPR)

Introduction

Ground Penetrating Radar (GPR) imaging is based on differences in the subsurface property of materials known as Relative Dielectric Permittivity (RDP). A GPR system transmits pulses of high frequency radio waves into the ground through a transducer or antenna. The transmitted energy is reflected when a radar pulse strikes a boundary where there is an abrupt change in RDP (Davis and Annan, 1989). A second antenna receives the reflected waves and stores them in the digital control unit. Subsurface objects are expressed as hyperbolic reflections similar to an inverted “U” shape. Targets are objects of contrasting permittivity and appear in plots as shaded hyperbolic shapes with the best definition when crossed at 90-degrees.

RDP controls, among other things, the velocity of the radio waves through the subsurface material; and, the wavelengths that the radio waves will have for different frequencies generated by different standard antennas; and, the shape or sharpness of the hyperbolic reflection described as signal spreading.

Values for RDP range from “1” at the low end, for air (fastest velocity), and “81” at the high end, for water (slowest velocity). Dry sand, wet sand, and saturated sand have RDP values of about 6, 15, and 25 respectively. The inverse relationship between RDP and velocity is important when estimating depths to targets based on shapes of the hyperbolic reflection. Examples of RDP ranges and effects include:

- Sand RDP = 9, speed = 0.1 m/ns causing broader, rounded, hyperbola;
- Wet Silt RDP = 16, speed = 0.08 m/ns causing more narrow, sharper, hyperbola.

Antenna selections are based on anticipated target depths and sizes. High frequency antennas are best for shallow depth and smaller targets like shallow pipes. Low frequency antennas are best for greater depth and larger targets, like geological and archeological applications. Examples of RDP effects on wavelength for a given antenna frequency include:

- Higher velocity / lower RDP (air, sand) = longer wavelength. Worse resolution, deeper depths.
- Lower velocity / higher RDP (wet silt) = shorter wavelengths. Better resolution, shallower depths.

Application of the Method

Draper Aden Associates (DAA) of Blacksburg, Virginia performed the GPR imaging surveys. DAA reports that field data were collected using the Noggin 250 manufactured by Sensors and Software, Inc. in Ontario, Canada.

The Noggin 250 utilizes a 250 MHz antenna mounted on a moveable cart. The Noggin 250 data were collected in grid fashion with parallel traverses in both the X and Y directions of the grid. Because of various site conditions in the study area, the effective depth of penetration of the 250 MHz GPR unit at the site was a maximum of approximately 24 feet.

As an added value, DAA elected to also use a Noggin 1000 with a 1000 MHz antenna mounted at the end of a long handle. The higher frequency utilized by the Noggin 1000 antenna provided a higher resolving power, but the depth of penetration was limited to approximately three to four feet. The benefit from using the higher frequency GPR is generally to provide information about asphalt and base layer thicknesses. In this case, the results were not useful with regard to evaluating local and global stability of the natural rock formation.

A 300 foot by 24 foot grid pattern was established for collecting 250 Hz GPR data over the width of the pavement along US Route 11 crossing Natural Bridge. Grid lines were spaced two feet apart in both directions of the grid, resulting in 12 lines along the long axis parallel to the road (Figure 5, top center).

Results of Ground Penetrating Radar Imaging

The results of the surveys are summarized below and described in detail in the appendix, *Geophysical Study at Natural Bridge*, pages 17 to 20; and in the accompanying figures shown on pages 49 through 60 in the appendix.

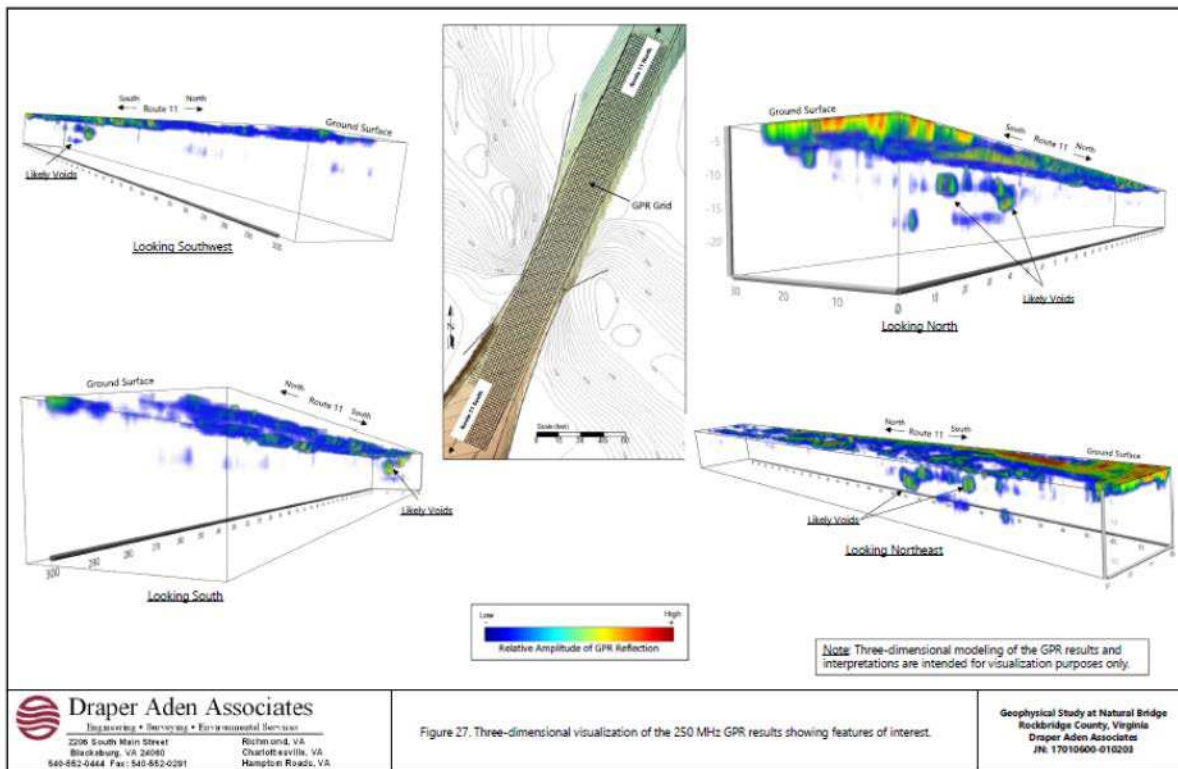
The 250 Hz GPR data were processed and presented by DAA in several different useful formats. For example, several figures in the DAA report illustrate all of the 250 Hz data as two-dimensional cross-sections, utilizing migration processing techniques that sharpen the GPR targets. Voids and bedrock pinnacles are visible that coincide with those identified using electrical resistivity imaging and seismic refraction profiling. Figure 5 shows the location of the GPR grid and four views depicting 3D modeling of all 250 Hz GPR lines. They also reveal numerous likely voids both within the rock formation itself and within the bedrock beneath approaches to the formation.

The following can be deduced from geological interpretations of the GPR imagery:

- a. Ground penetrating radar successfully imaged the uppermost layers of the rock formation and the highway approaches, including the pavement, base course material, and top of bedrock.
- b. These profiles are consistent with those from electrical resistivity imaging and

seismic refraction in that all indicate the presence of subsurface voids, although GPR does not extend as deep.

- These profiles also indicate the presence of cutter-and-pinnacle karst, consistent with the profiles from electrical resistivity imaging and seismic refraction.
- Analyses of these data indicate that the formation remains safe for the travelling public.



5. Unmanned Aerial Systems (UAS) General Photography and Videography

Introduction

Unmanned Aerial Systems (UAS), commonly called “drones,” refers to small robotic aircraft capable of carrying sensors of various types including standard cameras. The Radford University Geohazards and Unmanned Systems Research Center (RU) owns and operates more than six UAS’s in compliance with Federal Aviation Administration (FAA) regulations and Radford University UAS policies. The Research Center applied for, and was granted, permits from the Virginia Department of Conservation and Recreation (DCR) for flights within Natural Bridge State Park.

Mr. George Stephenson is RU’s FAA-Certified Remote Pilot in Command (FAA-RPIC). Several types of missions were planned as part of the investigation. They included

(1) manual flights for general photography and videography; (2) manual flights for oblique stereo photogrammetry; (3) device-assisted flights for oblique stereo photogrammetry; and, (4) pre-programmed autonomous flights for vertical mapping photogrammetry.

General photography and videography from the air is an effective tool for providing views from perspectives not normally seen. It often reveals completely new information, provides greater situational awareness that assists in timely decision making during investigations, and allows investigators opportunities to zoom in and out of key areas for greater detail.

Application of the Method

Radford University researchers used photography and videography from the air to (1) capture video imagery of the road alignment in relation to the natural rock formation orientation; (2) examine the area of pavement undercutting and erosion that was remediated in 2000 after rocks fell from it to the trail below; and, (3) to gather imagery from two sensitive rock block/slab locations for use in the safety factor calculations described below.

Results of General Photography and Videography

General photography and videography from the air can often be both revealing and dramatic. Figure 6 is a still image captured from high definition video of a mission flying downstream toward Natural Bridge. It shows how Route 11 crosses the rock formation at an angle, bringing the pavement very close to one of the most sensitive parts of the structure. A sensitive rock feature called “The Old Man” is circled. Above it are the concrete buttresses, marked by arrows, placed in 2000 to reduce undermining and erosion beneath the pavement.



Figure 6. Still image from RU UAS video looking downstream from the north. Shows orientation of Route 11 crossing Natural Bridge at oblique angle and proximity to sensitive features. "Old Man" structure is circled. Arrows indicate concrete buttresses placed in 2000 to reduce erosion and undermining beneath the pavement.

Figure 7 shows a close-up of the Old Man structure, the concrete buttresses, and an opening to one of the solution voids revealed by the electrical resistivity and GPR imaging. Figure 8 shows a close-up of a similar sensitive area on the downstream side of the rock formation.

The following comments pertain to the general aerial photography and videography. Data collection and analysis was performed by Radford University researchers.

- a. High resolution still photography and videos provide stunning views of the natural rock formation from perspectives not normally seen.
- b. Imagery highlights the diagonal alignment of the highway, crossing the natural rock formation at an angle that brings the edge of pavement within a few feet of the 215 foot drop, separated by a guardrail and wood fence, at the north-east end of the formation.
- c. High resolution imagery highlights potentially unstable rock masses that pose possible risks to park visitors on the trail below on both the upstream and downstream



Figure 7. Still image from RU UAS video. Close-up of sensitive areas of rock structure below the roadway. "Old Man" structure is circled. Arrows indicate solution void opening and concrete buttresses placed in 2000 to reduce erosion and undermining beneath the pavement.

- sides of the formation.
- d. High resolution imagery reveals exterior openings leading to the internal solution cavities identified in the electrical resistivity, seismic refraction, and GPR cross-sections.
- e. Analyses of these data indicate that the formation remains safe for the travelling public.



Figure 8. Still image from RU UAS video. Close-up of sensitive area of rock on the downstream-side of the rock formation. Low safety factor block is circled. Arrow indicates loudspeaker used during nightly sound-and-light shows.

6. Unmanned Aerial Systems Remote Discontinuity Mapping

Introduction

As introduced above, Radford University owns and operates more than six UAS's used for geohazards research. Several types of missions were planned as part of the investigation. Missions were flown on several different days under a variety of weather and lighting conditions.

This section highlights missions not described above. These missions were conducted primarily for the purpose of capturing imagery types needed for generating 3D point clouds for quantitative structural analysis. They include two manual flights for oblique stereo photogrammetry; and three device-assisted flights for oblique stereo photogrammetry.

Unmanned aircraft can be flown manually or autonomously in ways that capture hundreds of overlapping stereo images used to create 3D digital models. The models can exist in the form of point clouds containing hundreds of thousands of points, all with georeferenced coordinates in space and individual attributes, such as color, assigned to them. The point clouds can also be converted into digital triangle meshes that have a solid appearance on computer screens and which can be physically printed using 3D printers if desired.

Application of the Method

Radford University researchers flew three different types of small UAS aircraft at Natural Bridge as part of this study. They were (1) DJI Inspire 1 Pro; (2) DJI Mavic Pro; and, (3) 3D Robotics Solo. Missions conducted for 3D modeling purposes were flown both manually using stick and rudder techniques, with pilot-controlled camera shutter operation, and manually using stick and rudder techniques, with device-assisted camera shutter operation. During the latter, the aircraft system is programmed to take pictures at predetermined displacements of the aircraft, such as every 9 feet horizontally and 6 feet vertically, for example. The images were sorted for quality and processed using *Pix4D* software to produce georeferenced point clouds and triangle meshes. The point clouds were processed using *CloudCompare* software to extract discontinuity orientation data for stability analysis by Markland's Test on stereonets.

Results of Unmanned Aerial Systems Remote Discontinuity Mapping

The digital point clouds, triangle meshes, and data extracted from them are depicted in the following figures and plots. Figure 9 is a still image captured from a point cloud animation video showing the overall upstream-side point cloud. Figure 10 is an enlarged view and depicts the Old Man structure, the adjacent void opening, a through-cutting fracture, and the concrete buttresses beneath the pavement.



Figure 9. A still image taken from a point cloud animation of the upstream-side of Natural Bridge. Point clouds like this are georeferenced allowing for quantitative measurements to be made, including discontinuity orientations for stability analyses.



Figure 10. An enlarged view of the upstream-side of Natural Bridge, taken from the point cloud animation depicted above. The sensitive Old Man structure is circled. Arrows point to solution openings aligned with a through-cutting fracture. Point clouds like this are georeferenced allowing for quantitative measurements to be made, including discontinuity orientations for stability analyses.

Figure 11 depicts the discontinuity facets detected by the *CloudCompare* software and extracted from the point cloud of Figures 9 and 10, for stereonet plotting and stability analyses. This method of collecting geological structure data from point clouds reduces the need to rappel down slopes.

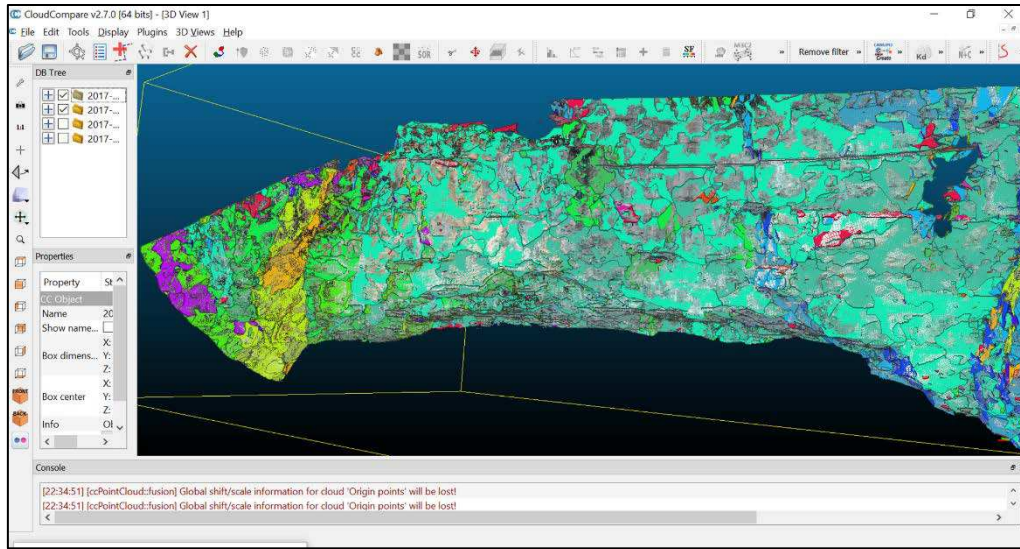


Figure 11. The point cloud shown in Figures 9 and 10 processed in **CloudCompare** software to extract discontinuity orientation values for stability analyses. Different colored facets or patches represent different sets of discontinuity orientations.

The following comments pertain in general to the unmanned aerial systems 3D mapping. Data collection and analysis was performed by Radford University researchers.

- a. 3D modeling of UAS stereo photogrammetry using the structure-from-motion (SfM) software package, *Pix-4D*, provided the highly detailed point clouds and triangle mesh models of both upstream and downstream rock faces.
- b. The 3D models are being used to extract discontinuity orientation data and plotted on stereonets, which reveal areas of unstable rock slabs and rock blocks on both upstream and downstream rock faces. These match areas identified by the photography and videography.
- c. These potentially unstable rock masses pose potential risks to park visitors on the trail below on both the upstream and downstream sides of the formation.
- d. The 3D models also confirm the presence of exterior entrances leading to the internal solution cavities identified in the electrical resistivity, seismic refraction, and GPR cross-sections.
- e. Stereonets extracted from the RU UAS 3D point clouds are provided for comparison manual discontinuity orientation data collection, and with studies conducted in 1999-2000.
- f. Analyses of these data indicate that the formation remains safe for the travelling public.

7. GigaPan Imaging

Introduction

GigaPan imaging systems basically consist of a robotic platform controlling a standard digital camera on a tripod so that very high-resolution overlapping images are captured from a single view point as the camera pans across a selected field of view. The images are then stitched together using specialized software to create a panoramic image of the subject containing extraordinary detail. The difference between GigaPan imagery and UAS overlapping imagery is that the camera view point is stationary for GigaPan and moving for UAS. UAS imagery is therefore more akin to a scan rather than a pan.

Application of the Method

Radford University researchers imaged Natural Bridge using a GigaPan system from five different vantage points on December 2, 2017. They included four pans looking up from various positions along the trail and one pan from the upstream observation point on the rock pinnacle across from the Old Man feature. An example of a still picture extracted from a GigaPan image is shown as Figure 12.

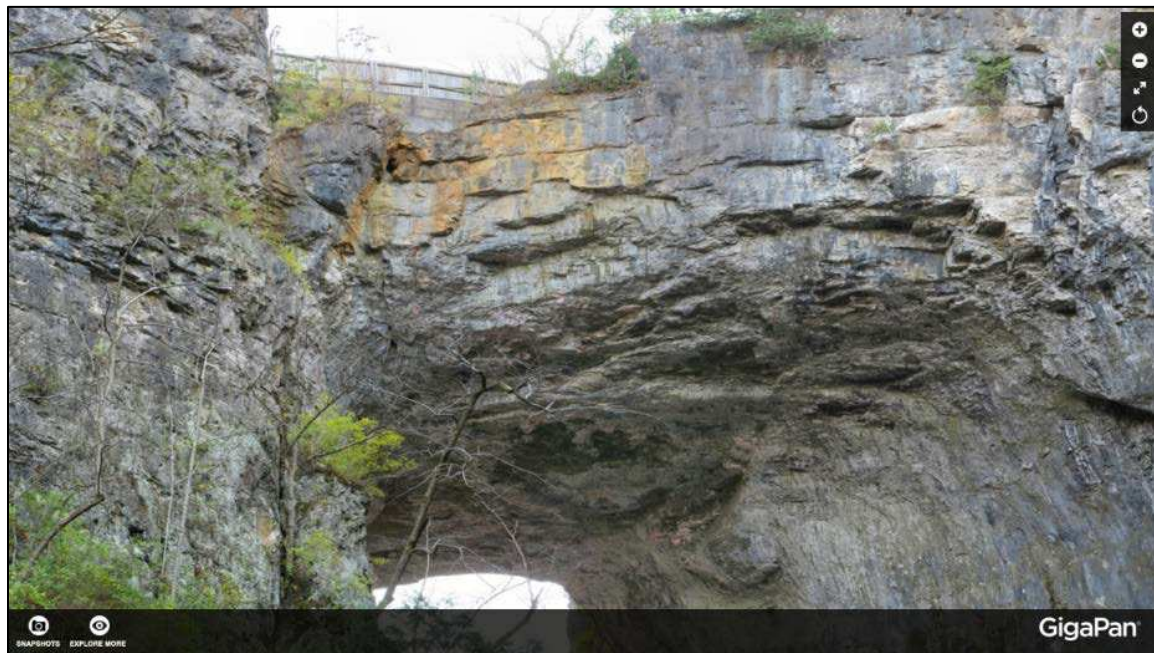


Figure 12. High resolution GigaPan image of the north side of Natural Bridge, normal zoom.

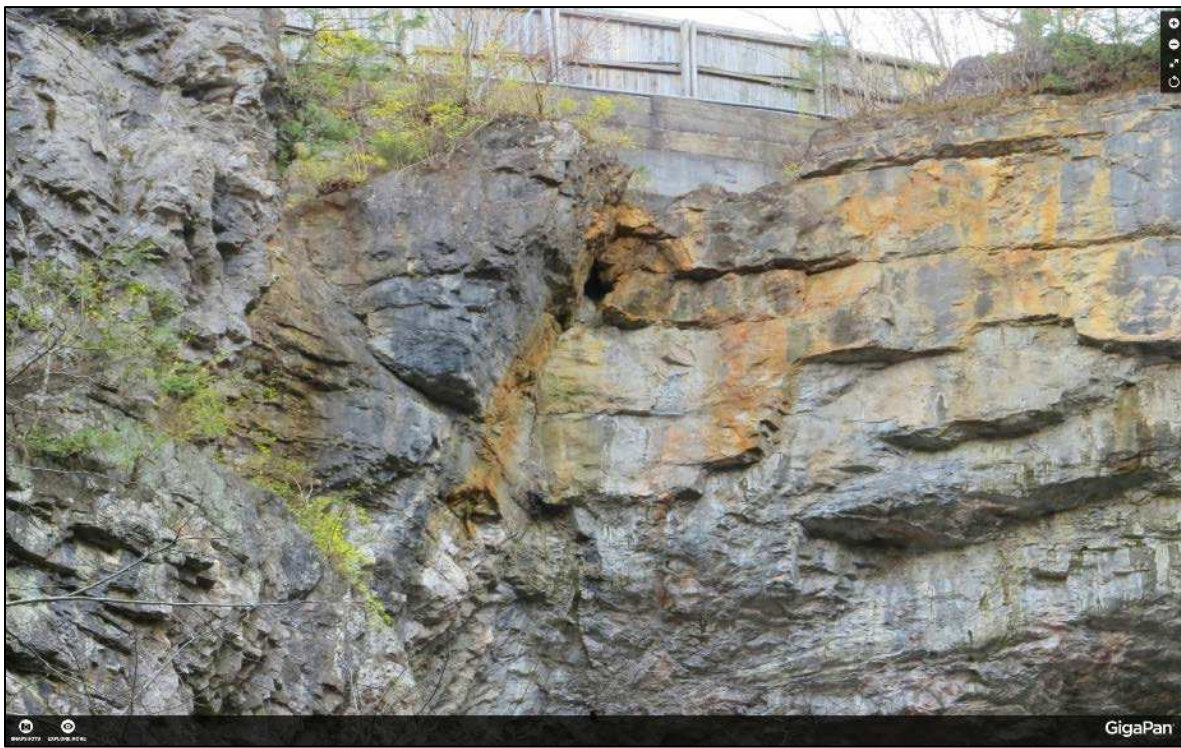


Figure 13. High resolution GigaPan image of the north side of Natural Bridge, zoomed in to show openings to solution voids.

Results of GigaPan Imaging

All of the GigaPan scans provide panoramic imagery of the formation in extraordinary detail. Figure 12 illustrates one of the most sensitive portions of the formation with regard to stability. Figure 13 is zoomed in to reveal greater detail of the through-cutting fracture surface to the side of the Old Man feature, including openings to the solution voids identified by the electrical resistivity imagery.

The following comments pertain in general to the GigaPan Imaging at Natural Bridge. Data collection and analysis was performed by Radford University researchers.

- a. The interactive high resolution GigaPan imagery provides close up zoom-able views of geological structure in the rock masses on both the upstream and downstream sides of the rock formation and Cedar Creek Gorge.
- b. The GigaPan imagery confirms the presence and the characteristics of geological structures and discontinuities recorded in the UAS photographs and videos.
- c. The GigaPan imagery confirms the presence and characteristics of geological structures and discontinuities identified in the digital 3D models, including the presence of exterior entrances to internal solution cavities.
- d. Analyses of these data indicate that the formation remains safe for the travelling public.

8. Terrestrial Light Detection and Ranging (LiDAR) for 3D Mapping

Introduction

LiDAR is a mapping system that uses a pulsating laser light to measure distances to targets. Terrestrial LiDAR uses an instrument mounted on a tripod on the ground as opposed to airborne LiDAR where the instrument is mounted in a manned, or sometimes unmanned, aircraft. The distance from the instrument to the target is determined by measuring the return time of the laser light pulse. Each return provides a coordinate in 3D space for a single point in the target area, along with information about the target, based on the intensity of the signal. Hundreds of thousands of points and their attributes are collected during a LiDAR scan creating a 3D point cloud as virtual representation of objects and surfaces within the scan area.

Application of the Method

Radford University undergraduate student researchers scanned Natural Bridge, using a Leica ScanStation C10 LiDAR system, from four different vantage points, on December 2, 2017. They processed the raw data using *Cyclone* software. The students simultaneously captured standard digital images with the C10 camera, which were projected onto the LiDAR 3D point cloud to optimize image visualization.

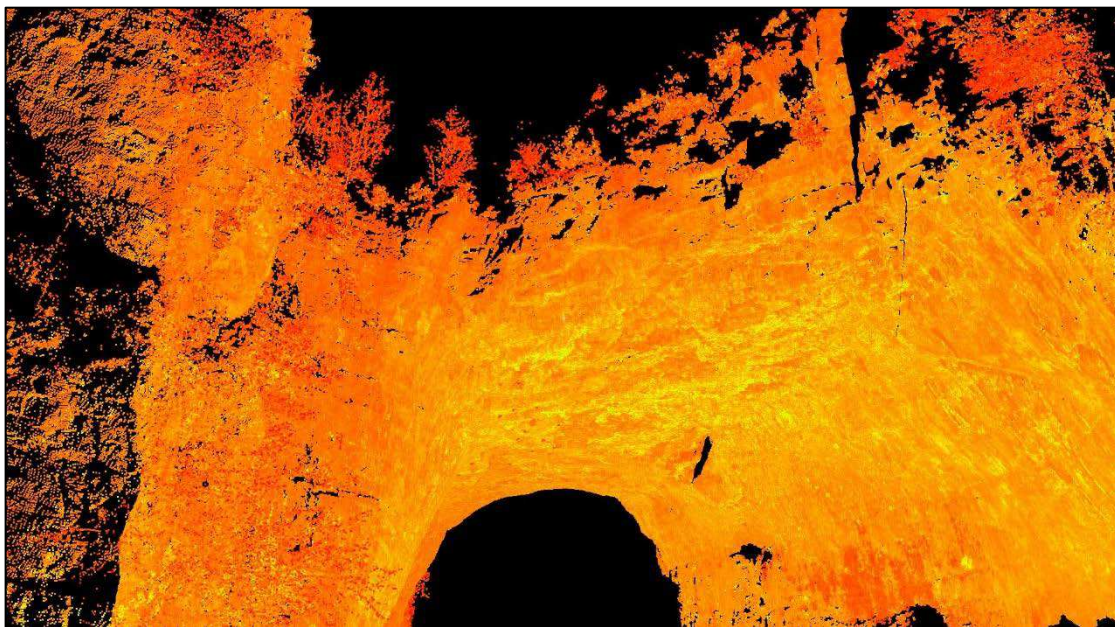


Figure 14. Example of LiDAR 3D point cloud generated by Radford University undergraduate researcher students.

Results of LiDAR Imaging

An example of a LiDAR point cloud generated using the Leica ScanStation is shown as Figure 14, above. As with the point clouds created from the RU UAS missions described above, the point clouds are scaled and georeferenced enabling quantitative

measurements to be made on the virtual 3D models. For example, distances, areas, and volumes can be determined, along with discontinuity orientation measurements. Programs such as *Split-FX* and *CloudCompare* allow stereonets to be plotted for kinematic stereonet stability analyses.

The following comments pertain in general to the LiDAR Imaging at Natural Bridge. Data collection and analysis was performed by Radford University researchers.

- a. Visual comparisons between the RU Terrestrial LiDAR imagery and the RU UAS 3D show that the point clouds are essentially identical for selected portions of the rock formation and the rock walls of the gorge.
- b. Because of time constraints, stereonets were extracted only from the RU UAS point clouds because they were generated from aerial viewpoints, providing useful perspectives not available in the terrestrial LiDAR data.
- c. VDOT also performed terrestrial scans at Natural Bridge using a similar LiDAR scanner. Dr. Brian Bruckno, VDOT, used *Split-FX* software to extract discontinuity orientation data from those point clouds and generated stereonet plots that corroborate those generated by RU using several different methods.
- d. These stereonets also agree with the discontinuity orientation data that were collected manually in 1999-2000, as part of the engineering geological study of the natural formation conducted at that time.

9. Manual Discontinuity Mapping

Introduction

Discontinuities are defined as breaks in the continuity of a rock mass that serve as weak zones, responsible for rock slides and rock falls, and as conduits for water flow. Documenting their orientations and physical characteristics is important to understanding and modeling the stability of rock features, like Natural Bridge. Most important are the directions these weak features are dipping, and the steepness of the dip angle, from 0° being horizontal to 90° being vertical.

Manual collection of discontinuity orientation data (Figure 15) was the standard for decades prior to the development of the LiDAR and UAS technologies that make remotely acquired, georeferenced, point clouds possible today. Often, manual data collection involved the use of rappelling ropes and the geological transit compass for measuring the dip direction and the dip angle of these weaknesses in the rock masses.



Figure 15. Manual collection of discontinuity orientation data by Radford University graduate students at Natural Bridge in 2000.

Manual data collection still involves direct access to rock faces and the use of geological compasses for confidence testing. However, smart phone applications now allow geologists to place their devices directly on geological features to automatically measure and store orientation data.

Application of the Method

During this study, an iPhone app called *GeoID* (Figure 16) was used to manually collect discontinuity orientation data rapidly. Data collection with *GeoID* involves placing the device on a discontinuity surface, allowing internal accelerometers to stabilize for a second or two, and pressing the data record button. A traditional geological transit compass was also used to validate the *GeoID* data. Data were collected at a variety of locations around the rock formation that are structurally similar by visual inspection to rock structures above the trail and out of reach.

The screen on the left shows typical discontinuity planar orientation data (**P**) in the form of *direction of dip / dip angle*. The screen on the right shows a stereonet indicating that the weak structures controlling the shape and orientation of Natural Bridge have a strong east-west, slightly northeast-southwest orientation.

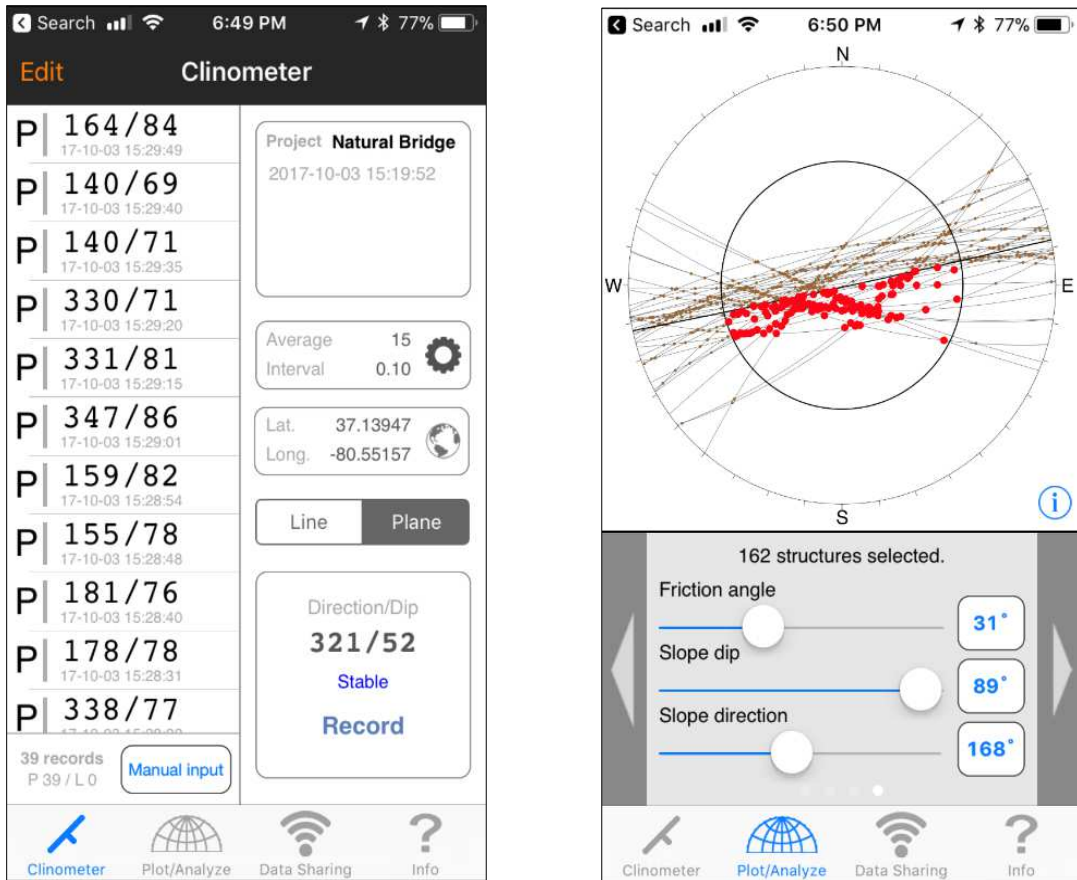


Figure 16. Sample screens from smart device application, GeolD, showing data collected at Natural Bridge in 2017.

Results of Manual Discontinuity Mapping

Manual discontinuity mapping in 2000, and today, resulted in structural weakness data for eight key areas. The discontinuity data can be displayed in several different ways. They are stored as numerical spreadsheets that include location information along with direction of dip and dip angle for each discontinuity measured. Additional parameters related to rock stability can be added as needed, including indications of water seepage and discontinuity type.

The simplest way to visualize discontinuity orientation data is to plot them on stereonets. In simplest form, stereonets may be thought of as compasses on which arcs representing planes of weakness may be plotted. The arcs are actually great circles. The alignment from end-to-end of the great circle on the compass corresponds to the real-world alignment of the weakness. And the straighter the great circle, the more steeply the weakness dips out of the rock mass. Conversely, the more curvature there is to the great circle, the less steeply the discontinuity dips out of the rock mass. Steep discontinuities are more dangerous than gently dipping discontinuities. Stereonet plots of the great circles, combined with representations of the slope geometry, allow for stability analyses to be performed. Figure 17 gives a sense of typical stereonets for Natural Bridge.

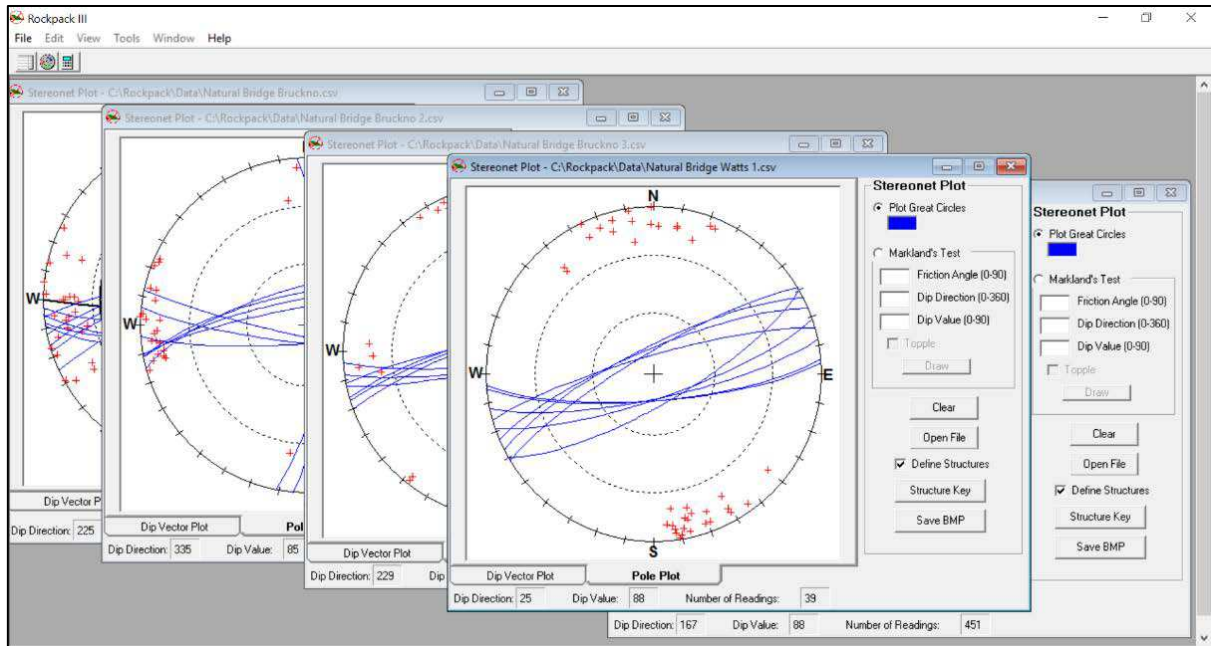


Figure 17. Sample stereonets for manually collected data from Natural Bridge in 2017.

10. Vibration Monitoring

Introduction

The effects of vibration on the stability of Natural Bridge are of concern with regard to short-term localized stability of individual rock blocks as well as to long-term global stability of the entire formation. Ground vibrations at Natural Bridge are primarily the result of cars and trucks passing over the formation throughout the day. Sound pulsations emanating from speakers hanging from stands mounted on the formation, for nightly sound-and-light shows, also contribute to the shaking.

Ground vibrations are evaluated with regard to (1) the frequencies of the vibrations; (2) the maximum rate of movement of the ground, in terms of Peak Particle Velocity (PPV) measured in inches per second; and, (3) the amount of acceleration (G's) that ground particles experience as they reach those peak velocities. Seismometers typically record the frequencies and the amplitude of vibrations from which the peak particle velocities and particle accelerations can be calculated. Accelerometers directly record the acceleration of the ground from which peak particle velocities can also be calculated.

To evaluate the short-term effects, each vibration event is treated as a minuscule force pushing on components of the rock mass. The forces are calculated from the ground acceleration values and added to other driving forces for calculating safety factors, described in the next section. If resisting forces are equal to driving forces, then the rock block is said to be at equilibrium and has a safety factor of 1.0. A safety factor greater

than 1.0 indicates that the resisting forces are greater than the driving forces and the area should be safe. Safety factor values that become too low, that is, those that drop to near 1.0, are cause for concern.

In the long-term, recurring vibrations place repetitive stress on sensitive components of the formation and will reduce stability over time. In recent years, Strength Reduction Factor (SRF) methods for evaluating rock slope stability have become standard as way to examine the impact of strength degradation within rock discontinuities on global stability. SRF methods include reducing any one of several strength factors (for example, shear strength) in any number of slope stability equations, reducing the factor until theoretical failure occurs. This determines the critical strength reduction factor (critical SRF), or safety factor, of the slope. The effect of each individual vibration event, on long-term global stability, is difficult to quantify as the exact strength reduction values cannot be measured.

Application of the Method

Three different types of vibration sensors have been deployed at Natural Bridge in various locations and have produced results similar to each other. Included are: Infiltec QM-4.5V-20HZ vertical seismometers; Radford University Model 03 triaxial accelerometers; and; VibSensor triaxial accelerometer application version 2.0.0 on three iOS smart phones.

These devices are extremely sensitive to vibrations and are documented to have sensitivities on the order of thousandths of a “G” (Amick, et al., 2014), where “G” represents the Earth’s gravitational pull. The most useful of these sensors thus far at Natural Bridge have been the *Infiltec QM-4.5V-20HZ* vertical seismometers. Examples of results from the *Infiltec* are presented here.

Results of Vibration Monitoring

Vibrations from traffic are easily detected on the rock formation near the highway and at sensitive rock locations above the hiking trail as far as 100 feet from the highway. There also appeared to be low amplitude continuous vibrations of an unknown origin at this time. They may be related to a nearby water treatment facility or to HVAC equipment at the hotel and visitors center.

Vibrations from speakers, hanging from supports mounted to the rock mass at two locations, were also observed during a sound-and-light show on December 22, 2017. However, since traffic was not stopped during the program, it is not possible for us to separate the traffic vibrations from the speaker vibrations in the seismographs at this time. In order to most accurately assess the speaker vibrations, it would be necessary to either close the road during a performance, or carefully monitor which vibration signals relate to traffic and which relate to sound during a performance.

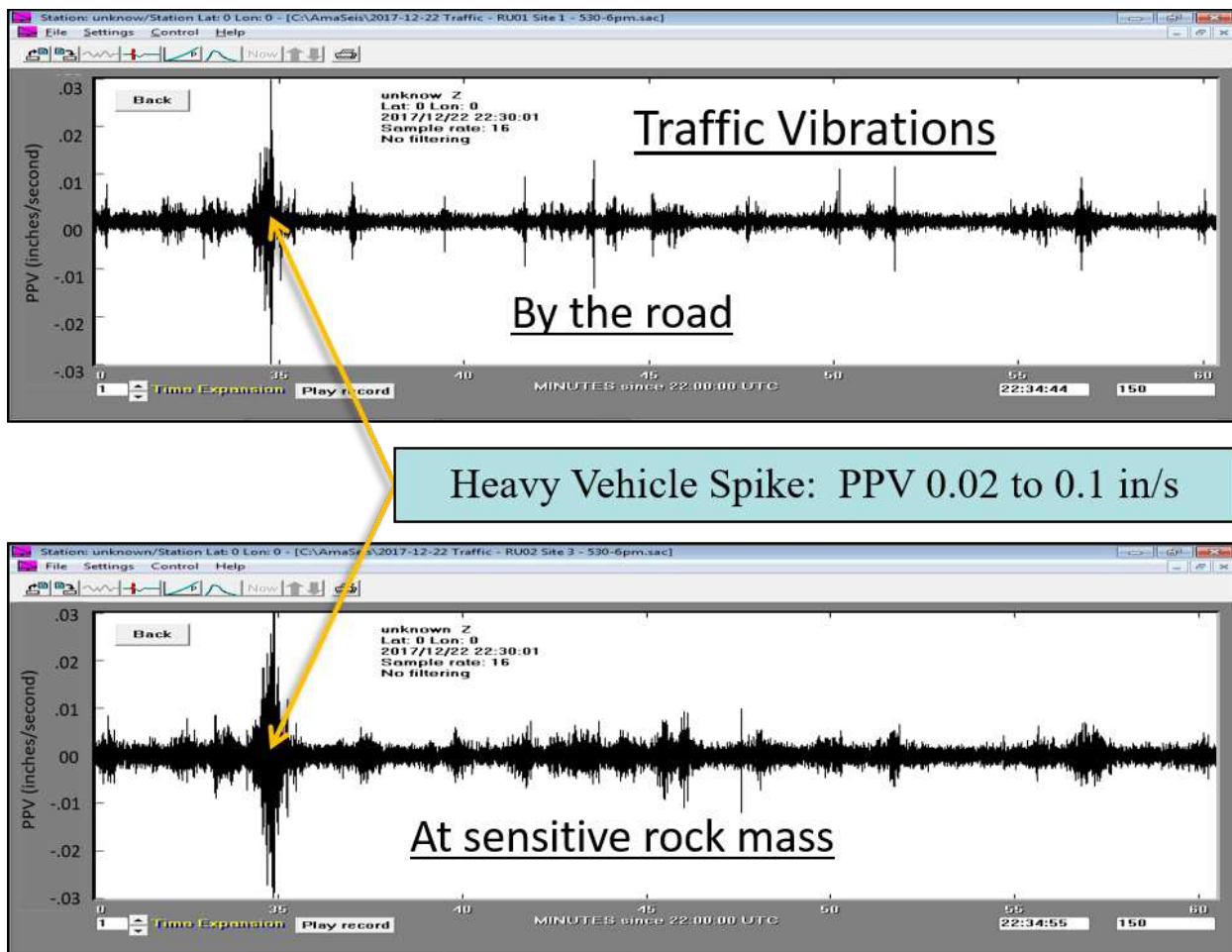


Figure 18. Typical traffic seismograms for a thirty-minute period at Natural Bridge during the evening of December 22, 2017. Top graph represents a seismometer next to the highway. Bottom graph represents a seismometer approximately 110 feet away from highway centerline, on a sensitive rock block. Sensitive rock masses appear to resonate for a longer period of time than the earth adjacent to the highway.

Figure 18 shows typical seismograms for normal traffic conditions. A spectral analysis of several seismograms for traffic at Natural Bridge reveals that the average frequencies are 6.46 Hz (cycles per second), with PPVs ranging from 0.028 inches/second to about 0.095 inches/second, or essentially 0.10 inches/second.

Putting those values into perspective with regard to human sensitivity, a value of 0.02 inches/second is considered to be the threshold of perception; 0.08 inches/second is readily perceptible; and, 0.10 inches/second becomes annoying to individuals (Caltrans, 2013).

With regard to manmade structures, continuous vibrations with PPVs of around 0.02 inches/second are unlikely to cause damage; while the value of 0.08 inches/second is the recommended upper limit to which ruins and ancient monuments should be subjected; yet, values around 0.10 are believed to pose virtually no risk of damage to normal buildings (Whiffen, 1971).

For comparison, Todd Beach of VDOT, reported peak particle velocities of 0.06 inches per second adjacent to the highway on Natural Bridge during traffic vibration studies in 2000 (Watts, et al., 2000). Those values were recorded directly above concrete buttresses protecting one of the most delicate portions of the rock formation; the equipment used at that time was less sensitive than the equipment used in the current study.

Significantly, sensitive rock slabs on the sides of the rock formation were recorded to resonate from vibrations longer than did areas directly adjacent to the highway. Considering the values presented above, it is fair to say that the rock comprising Natural Bridge is affected by these vibrations, but not to an extent likely to cause immediate damage or instability. Vibration effects are included in the stability modeling and safety factor analyses of the following section.

11. Local Safety Factor Calculations

Introduction: Local Stability versus Global Stability

Assessing the safety and stability of rock masses is often divided into two categories, those being the global catastrophic failure of a large feature, in this case, the collapse of Natural Bridge and the road it carries, and smaller localized failures of portions of the rock formation. Both types of failure can be dangerous to the public.

This section addresses the smaller localized failures such as rock falls, rock slides, and rock topples. In 1999, a tourist standing beneath Natural Bridge was killed by the localized fall of a rock slab from beneath the formation.

Two steps are normally involved in evaluating the localized safety of rock structures whenever stability is controlled by geological discontinuities, as it is at Natural Bridge. They are (1) kinematic stereonet analysis and (2) safety factor calculations by limiting equilibrium and strength reduction factor methods.

The first step examines discontinuity orientation data to identify geometries that could lead to unstable conditions. This is accomplished by plotting the structural discontinuities and slope geometry on diagrams called stereonets and performing kinematic analyses. Unfavorable orientations exist when points plot in certain critical zones on the stereonets. The critical zones reveal geometries that might lead to sliding of rock blocks on weaknesses, or combinations of weaknesses that might create unstable rock wedges, or rock blocks that might topple out of the rock face.

After unfavorable geometries have been identified on stereonets, the second step is to quantify how unsafe those potentially unstable areas may be using safety factors. The concept is simple, acquiring all of the strength parameters is not so simple. Engineering software can be used to estimate the resisting forces and the driving forces that are acting

on specific rock blocks. Those forces are then compared to each other as simple ratios. If resisting forces are equal to driving forces, then the rock block is said to be at equilibrium and has a safety factor of 1.0. A safety factor greater than 1.0 indicates that the resisting forces are greater than the driving forces and the area should be safe.

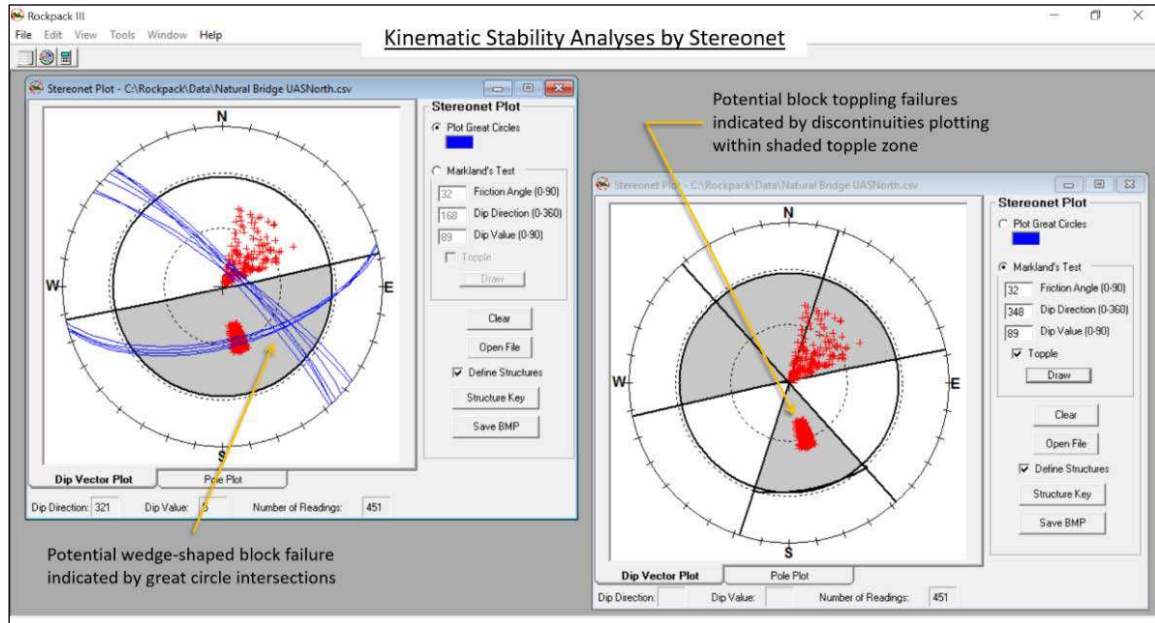


Figure 19. Examples of stereonets created as the first step in stability analyses at Natural Bridge. Plot on the left reveals the possibility of rock wedge failures on the south side of the bridge. Plot on the right reveals the possibility of toppling failures into the gorge on the on the north side of the formation.

Application of the Method

(1) Kinematic Stereonet Analyses

Figure 19 shows just two examples of the dozens of stereonets that could be used to evaluate the stability of different portions of the rock faces that make up Natural Bridge. Very simply put, the kinematic stereonet analysis of Figure 19 compares the orientations of the discontinuity weaknesses, obtained by LiDAR, UAS 3D modeling, and manual data collection, with the actual physical geometry of the rock faces at Natural Bridge. The arrows point to stereonet indicators of potential rock wedge failures in the diagram on the left and potential rock toppling failures in the diagram on the right.

(2) Safety Factor Calculations

Figure 20 depicts the standard safety factor calculations for a rock slab on a steep slope. Input parameters such as *weight* and *angle of sliding surface* are derived from our extensive 3D mapping data and stereonet analyses. Those values contribute to driving

and resisting force determinations, along with estimates of discontinuity strength values, from previous laboratory testing and values published for similar rocks and structures.

Due to inherent uncertainties in measurements and strength values, safety factors of at least 1.25 are typically considered necessary along highways. Greater values are even more desirable whenever possible. It is important to realize that safety factors will decrease over time as discontinuities weather and rocks become weaker.

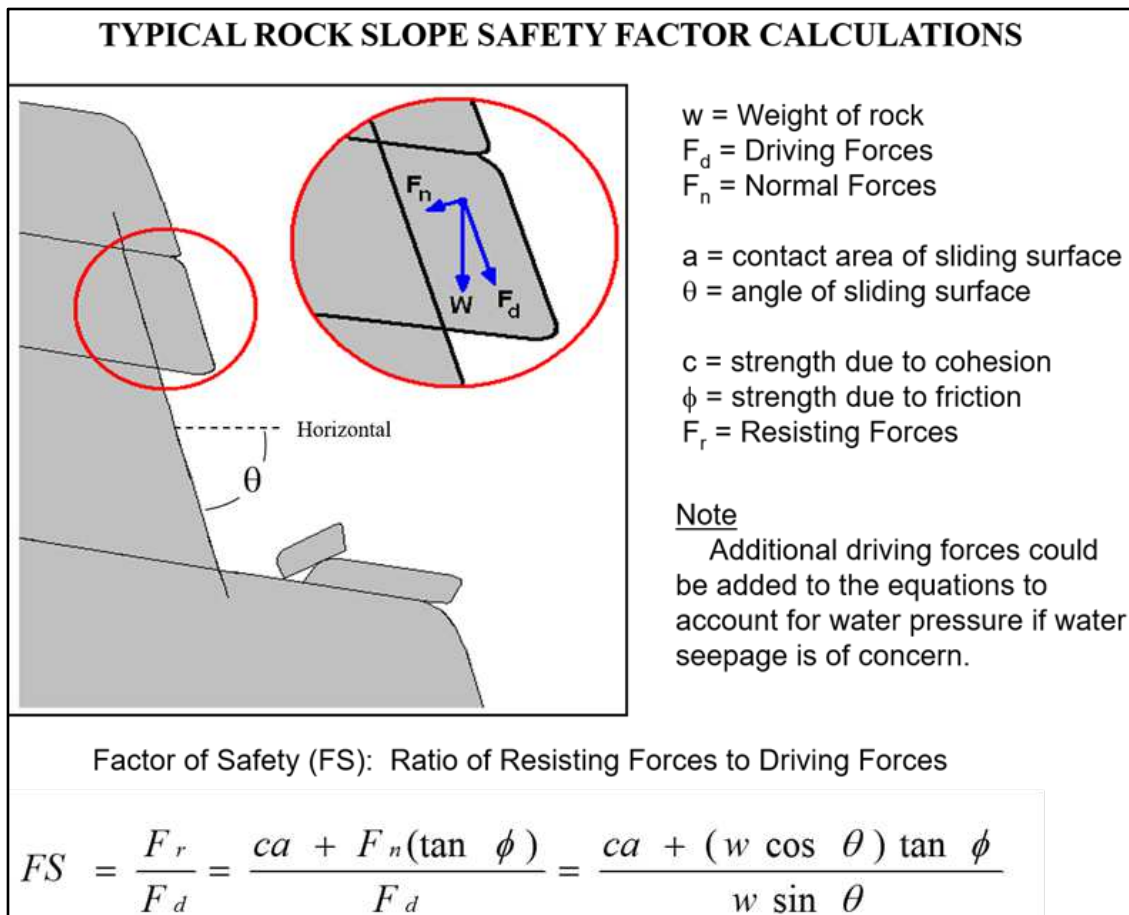


Figure 20. The general safety factor equation for rock slope stability (Watts, 2012). Neither the role of water nor the role of vibration as additional driving forces, are included in these sample equations.

Results of Local Stability Modeling and Safety Factor Calculations

Figure 21 shows the final step in the stability analysis of a rock block in the vicinity of the Old Man structure on the north side of the rock formation showing the last step in a worst-case scenario; the Old Man is believed to be most sensitive of the sensitive structures.

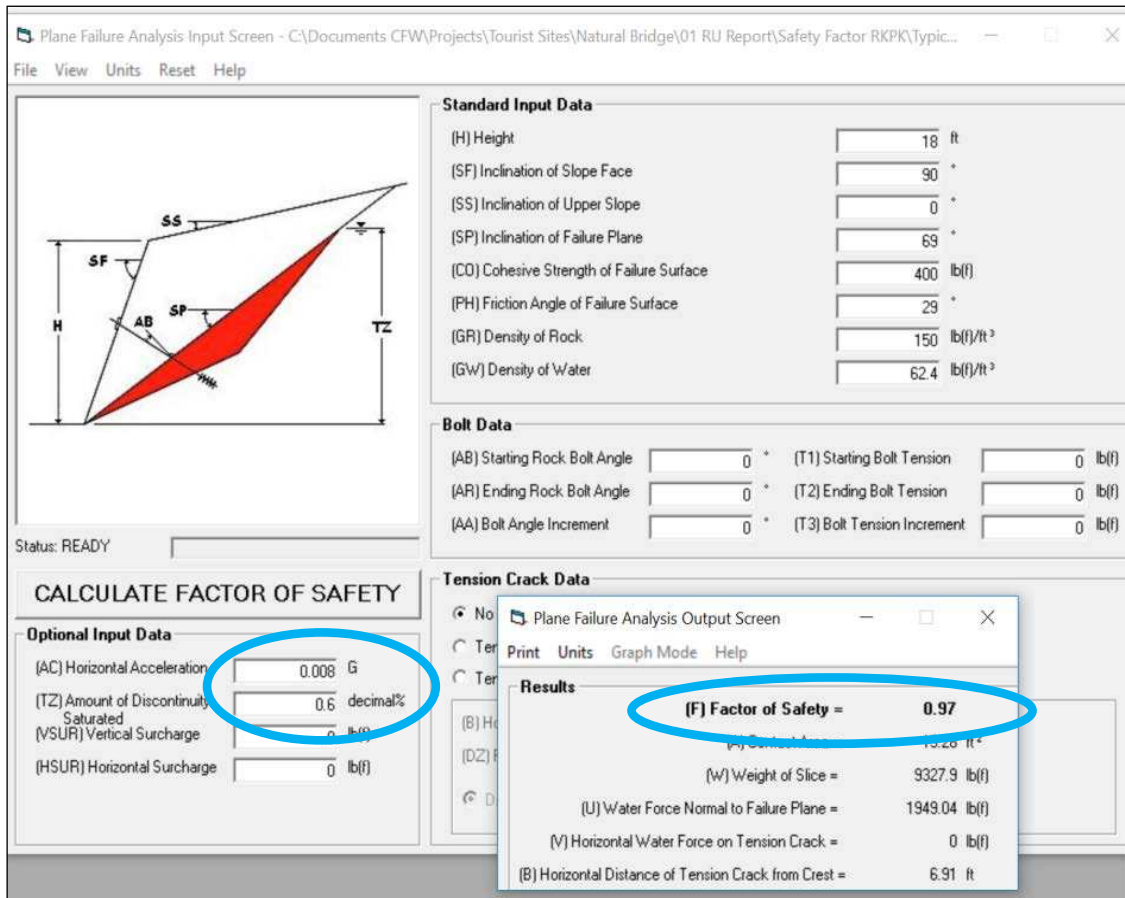


Figure 21. Example of a safety factor calculation using RockPack III software from RockWare. Note that in this worst case scenario, a vibration of 0.008 G, while the weak discontinuity surface is partially saturated, causes the safety factor to drop below 1.0, to 0.97. This would most likely result in a rock fall.

In Step One of this worst-case or near-worst-case scenario, the factor of safety without vibrations or water seepage would be 1.1. That is theoretically safe, although very close to the equilibrium value of 1.0, making it a “sensitive” location. Adding vibration to the stability analysis as another driving force is straightforward as is adding water pressure as another driving force. For example, if a vibration of 0.008 G is added to this case, the local short-term safety factor drops to 1.09, which is even less stable than for the static condition. Greater vibrations would further lower the factors of safety. Finally, if the discontinuity becomes partially saturated, to 60% for the 0.008 G case, the safety factor drops below 1.0 to 0.97, suggesting that a rock fall would be imminent. It should be noted that most natural geological formations, such as rock and soil slopes, generally hover near a factor of safety of 1.0, and are therefore dynamic in nature and behavior, making Natural Bridge and its environs typical in this sense.

Vibrations can impact rock slope stability in two ways. In addition to increasing short-term driving forces, as calculated above, continuous repetitive vibrations will aggravate the long-term natural reduction of discontinuity strength, thus reducing the resisting forces over time.

The stability of rock masses is controlled by the strength of the weakest discontinuities. Natural processes of weathering, erosion, and gravity are always at work weakening bridges or patches of intact rock that hold discontinuities together. These patches are very much like rusting bolts holding together a traditional bridge. The more bolts that break, the less stable the traditional bridge becomes. Recurring vibrations hasten the weakening of these rock patches, reducing both short and long-term stability.

Summary of Local Stability Analyses

- a. Kinematic stereonet tests reveal potentially unstable rock slabs and rock blocks on both the upstream and downstream sides of the natural rock formation and the rock walls of the gorge.
- b. Safety factor computations, taking into account geometries from 3D point clouds, discontinuity orientations, and discontinuity shear strength estimates indicate that rock falls and rock slides are very likely over time onto the trail within the gorge and beneath the rock formation.
- c. Computer models estimate that the safety factor of the rock feature known as the Old Man is near equilibrium with a value of 1.10, without considering vibration. This is lower than the typically desired value of 1.25 to 1.30 for highway rock slopes.
- d. The addition of vibration data collected at Natural Bridge provides an estimated decrease in safety factor from 1.10 to 1.09.
- e. The addition of partially-filling cracks with water reduces the safety factor to the unsafe value of 0.97.

12. Global Safety Factor Calculations

This section addresses global failures, or those failures caused by large, through-cutting features such as joints or other fractures. These failures typically result in large, often catastrophic failures and, in the case of Natural Bridge, would likely render the structure unsuitable for use as a transportation, or even pedestrian, corridor.

Radford University developed a mathematical model for the global stability analysis. This involved selecting the most likely mechanism for failure along a through-cutting, nearly vertical fracture, using published values for a range of shear strength values, modeling the geometry of the formation, and selecting a reasonable range of annual strength reduction (SR) values where strength reduction is the result of natural weathering.

The mathematical model suggests that the geological structure should be stable and free from global failure for a time period in the range of 5,000 years to 14,400 years. The results are presented in Table 1, below:

Time to Global Failure based on strength reduction rates

SR/yr =	0.72	psf/yr	Time =	5,000.00	yrs
SR/yr =	0.50	psf/yr	Time =	7,200.00	yrs
SR/yr =	0.25	psf/yr	Time =	14,400.00	yrs

Table 1: Time to Global Failure based on strength reduction rates (SR/yr), where shear strength is measured in pounds per square foot (psf).

The mathematical model above is likely the worst-case scenario for global stability. Geomorphological models, including carbonate solution rates and rates of natural weathering (including weathering caused by local failures) are thought to be an order of magnitude greater than mathematical models. However, calibrating geomorphological models to generate a landscape-evolution prediction of global stability requires collecting data over the course of several years and is therefore beyond the scope of this report.

SUMMARY OF RESULTS

1. Internal Structure

Geophysical surveys, including electrical resistivity imaging, seismic refraction, and ground penetrating radar, indicate that the rock formation comprising Natural Bridge contains solution voids and that the depth to bedrock is variable due to cutter-and-pinnacle karst.

2. External Shape and Structure

External surveys, including manual discontinuity mapping, LiDAR scans, and 3D photogrammetry from unmanned aerial systems, indicate that the general external shape and orientation of Natural Bridge is controlled by typical geological structures that strike generally east-northeast. Those discontinuities provide a preferential grain to separations in the rock mass and are primarily bedding planes, joint sets, and at least one through-cutting fracture. Small external openings are visible in the imagery that lead into the rock formation toward the solution voids revealed by the geophysical surveys.

3. Vibration Analyses

Seismometers (vibration sensors) were placed at Natural Bridge to detect small vibrations from traffic and other sources close to the pavement and on sensitive rock features with low safety factor values. The seismograms indicate that the vibrations resonate longer on the sensitive rock features than on solid ground next to the highway. The effect of vibrations in the long-term is to aggravate the natural deterioration of strength parameters associated with discontinuities. The effect of vibrations in the short-term is to add pulses of energy to rock masses in the form of short driving forces. These pulses cause decreases in stability for the duration of the pulse.

CONCLUSIONS AND RECOMMENDATIONS

- Analyses of these data indicates that the formation remains safe for the travelling public for the lifespan of a typical transportation corridor.
- Results indicate that the rock formation has internal solution cavities, but they do not suggest any overall instability of the geological feature. These are typical cavities found everywhere in karst terrain typical of limestone bedrock.
- Of greatest concern are the naturally occurring weak areas on the sides of and beneath the rock formation and the gorge. These are visible in UAS drone photography, 3D digital point cloud models generated by the UAS stereo photogrammetry along with LiDAR, and in the GigaPan interactive imagery. These weak areas will result in occasional local rockfall events. While these do not directly or immediately affect the global stability of the geological feature, they potentially pose a rockfall risk. Risk mitigation strategies are available; however, these strategies require that local failure data be collected and analyzed and calibrated to the specific locality. As these data require substantial time to collect, this is beyond the scope of this report at this time, but may be completed as a future task. It is recommended that local rockfall risk be evaluated and risk mitigation strategies be developed.
- Pseudo-static computer modeling of vibrations indicate that they will negatively impact the naturally occurring weak areas over time.
- Geophysical investigations, specifically electrical resistivity imaging, seismic refraction, and ground penetrating radar show solution voids in the bedrock that would contraindicate construction of a manmade bridge over the natural formation as a possible solution to the detrimental effects of traffic vibrations.
- Natural weathering and human activities will eventually reduce the suitability for vehicle traffic.
- Initiating measures to reduce water infiltration may be considered as an interim measure to increase safety.
- Due to the engineering geological condition of the rock formation, altering existing stress fields and load conditions by building a new, manmade bridge over Natural Bridge is not recommended.
- It is recommended that vehicular traffic be eventually removed from Natural Bridge according to VDOT's regular development, planning, and engineering processes.

ACKNOWLEDGMENTS

The authors wish to thank the following individuals for their significant contributions to the successful completion of this investigation.

- Dr. Brian Bruckno, Engineering Geologist, Staunton District, Virginia Department of Transportation
- Superintendent Jim Jones and Chief Ranger Dale Davis, Natural Bridge State Park, Virginia Department of Conservation and Recreation
- Mr. Ted Dean, Mr. Chris Printz, Ms. Johanna Vaughan, and Mr. Ethan Truman, Draper Aden Associates, Blacksburg (Geophysical Investigations)
- Mr. Chris Mau, Ms. Cassandra Wiggins, Radford University (Unmanned Aerial Systems flights and data processing)
- Dr. Parvinder Sethi, Dr. Ryan Sincavage, and Ms. Rebecca Norton, Radford University. (GigaPan imaging)
- Mr. Colby Ryan, Mr. Joseph Spriggs, and Mr. Levi Dollarhite, Radford University. (LiDAR)
- Dr. Rhett Herman and Mr. Ross Robertson, Radford University. (RU vibration sensor development and testing)

REFERENCES

Amick, R.Z., Patterson, J.A., and Jorgensen, M.J., 2013. Sensitivity of Tri-Axial Accelerometers within Mobile Consumer Electronic Devices: A Pilot Study, *International Journal of Applied Science and Technology* Vol. 3 No. 2.

Bourbié, T, Olivie Coussy, and Bernie Zinszner, 1987. Acoustics of Porous Media, Gulf Publishing Company, 334 pp.

Caterpillar, Inc., 2000. Handbook of Ripping, Twelfth Edition, Peoria , IL.

Davis, L. and Annan, A.P., 1989. Ground-penetrating radar for high-resolution mapping of soil and rock stratigraphy. *Geophysical Prospecting*, Vol. 37, pp. 531-551.

Griffiths, D.H. and R.F. King, 1988. Applied Geophysics for Geologists & Engineers: The Elements of Geophysical Prospecting, Pergamon Press, 230 pp.

Matthews, M. C., Hope, V. S., and R. I. Clayton, 1996, The use of surface waves in the determination of ground stiffness profiles, *Proceedings of the Institution of Civil Engineers in Geotechnical Engineering*, Vol. 119, April, Pages 84-95.

Spencer, E.W., 1968, Geology of the Natural Bridge, Sugarloaf Mountain, Buchanan and Arnold Valley quadrangles, Virginia: Virginia Division of Mineral Resources, Report of Investigations 13, scale 1:24,000.

Watts, C.F. and Gilliam, D.R, 2000. Engineering Geologic Evaluation of Rock Slope Stability at Natural Bridge, Virginia, a report prepared on behalf of Natural Bridge of Virginia, 24 pp.

Watts, C.F., Underwood, S.A., Haneberg, W.C., and Rogers, J.D., 2012. Fully rationalized equations for incorporating joint water pressure in rock slope stability analyses at Glacier Point in Yosemite National Park, California. *Landslides and Engineered Slopes: Protecting Society through Improved Understanding*, 2, 1173-1178.

Whiffen, A.C., 1971. A Survey of Traffic-induced Vibrations, Crowthorne, Berkshire : Design Division, Road Research Laboratory

APPENDIX

GEOPHYSICAL STUDY
FOR NATURAL BRIDGE
Rockbridge County, Virginia

December 6, 2017

Draper Aden Associates
Blacksburg, Virginia